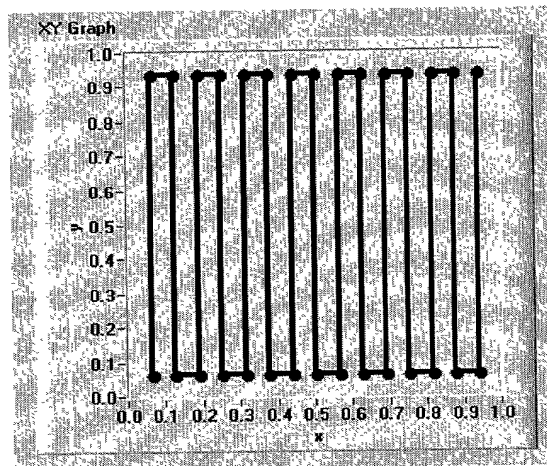


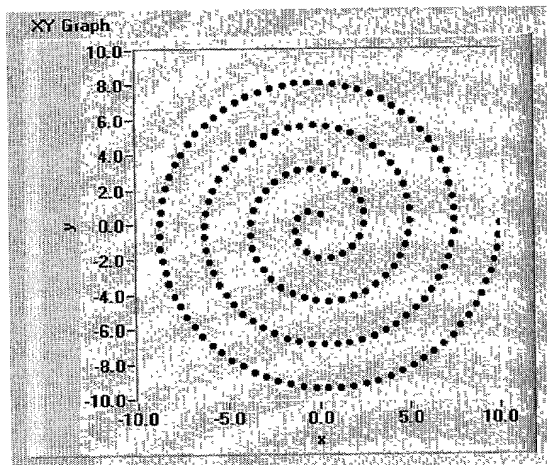
Approximated Peano Curve. The space-filling process has not been completed.

Figure 1A (Prior Art)



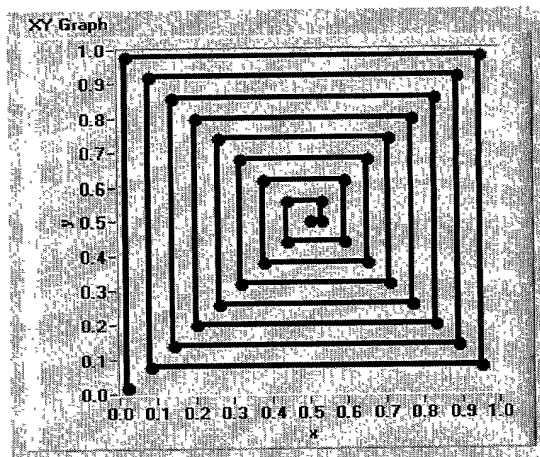
Boustrophedon Path

Figure 1B (Prior Art)



Archimedes Spiral defined by equally distributed points

Figure 1C (Prior Art)



Spiral-like line-based scanning

Figure 1D (Prior Art)

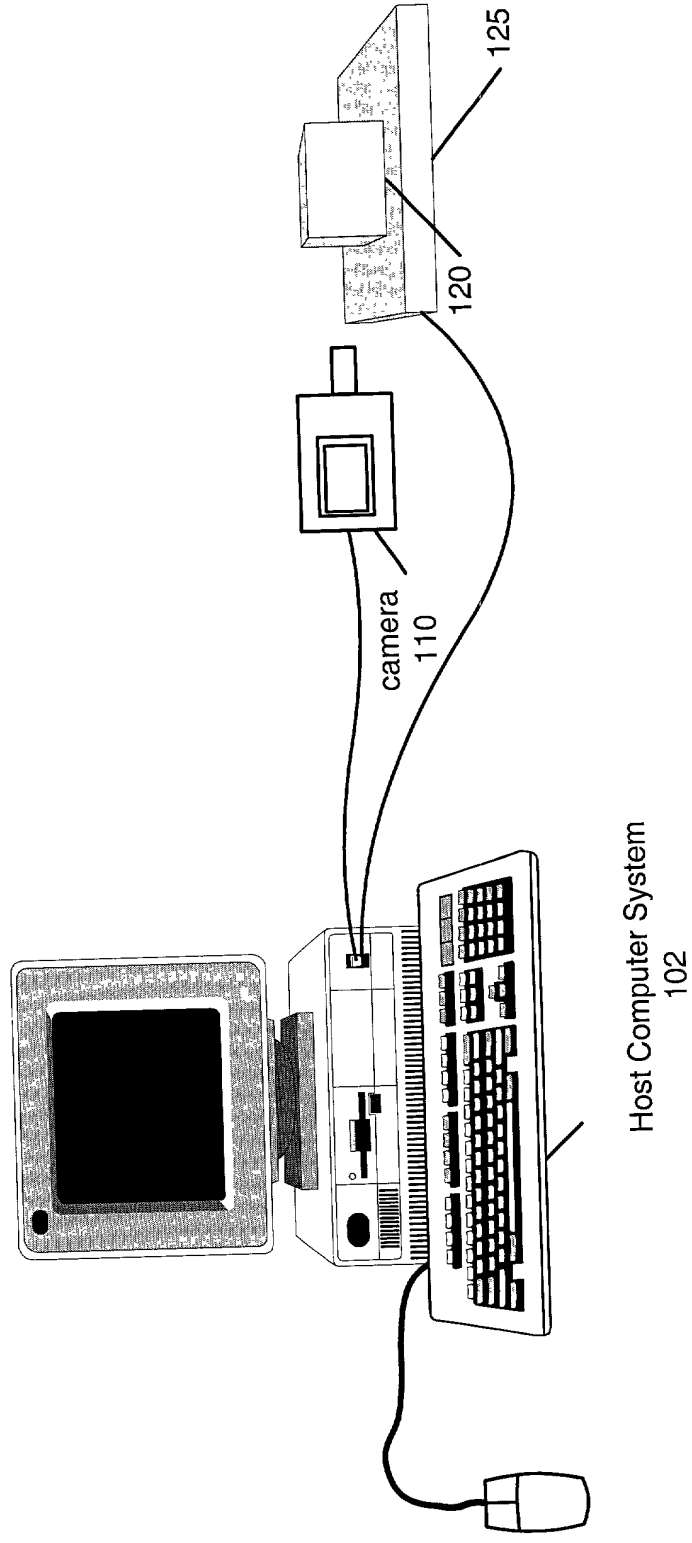


Figure 2A

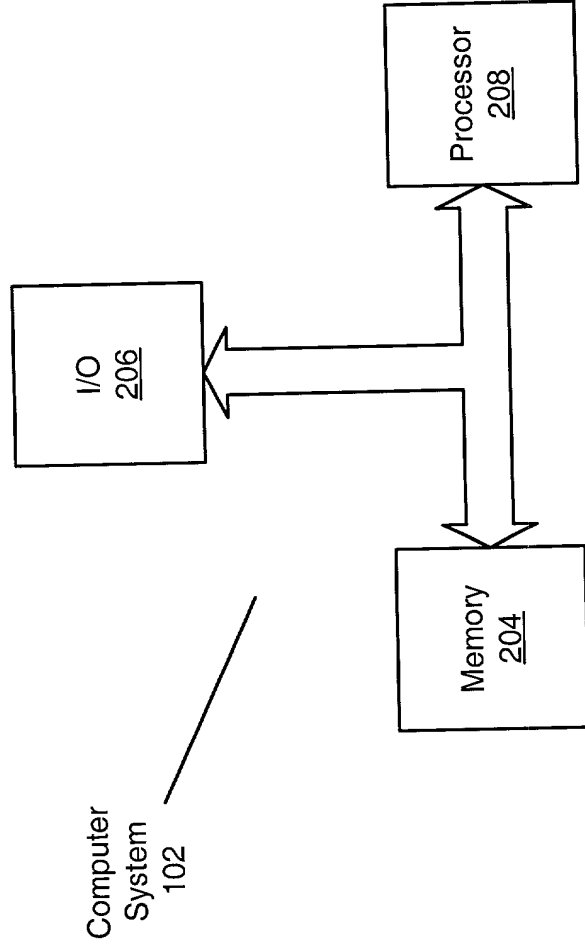


Figure 2B

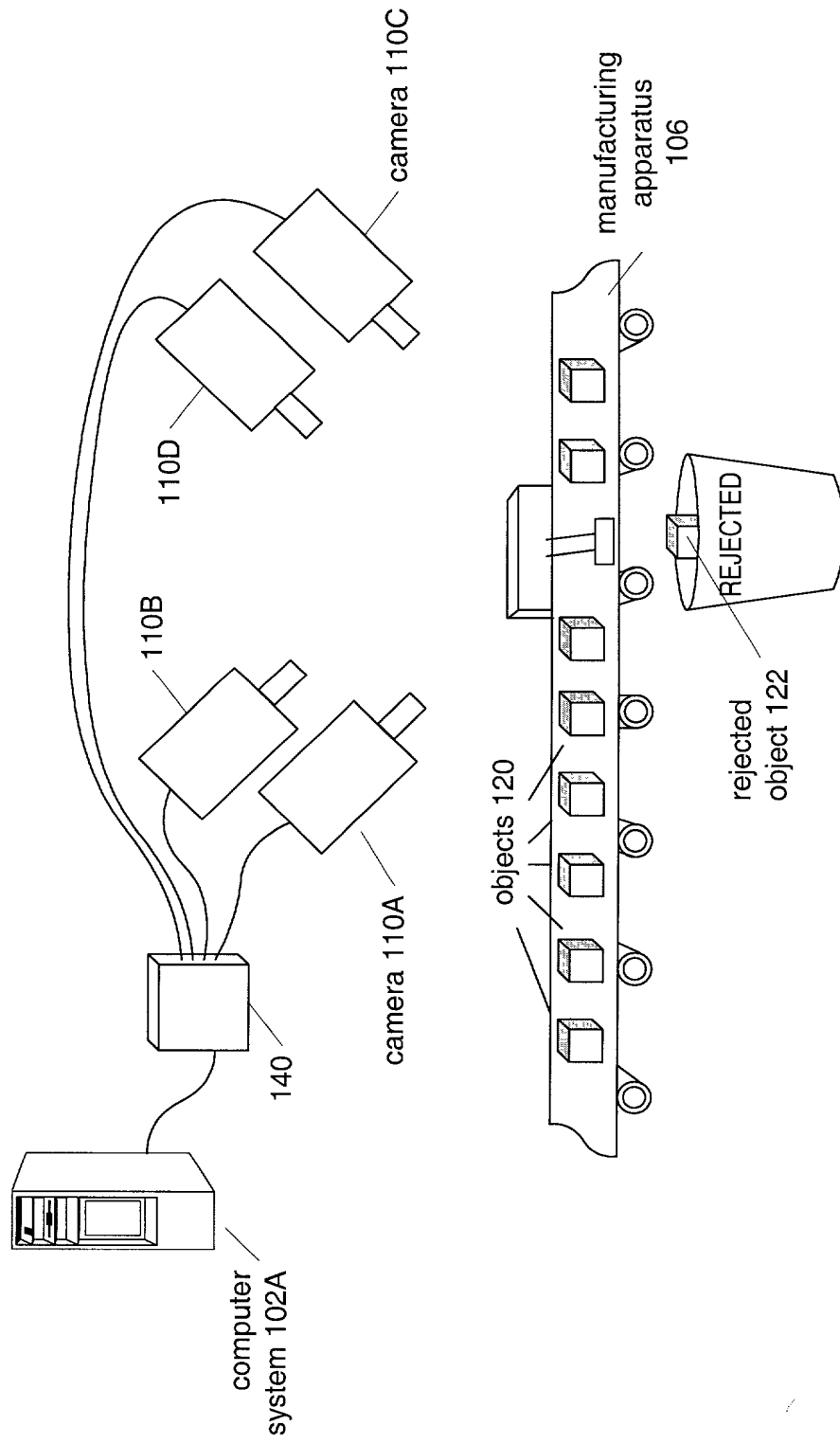


Figure 3A

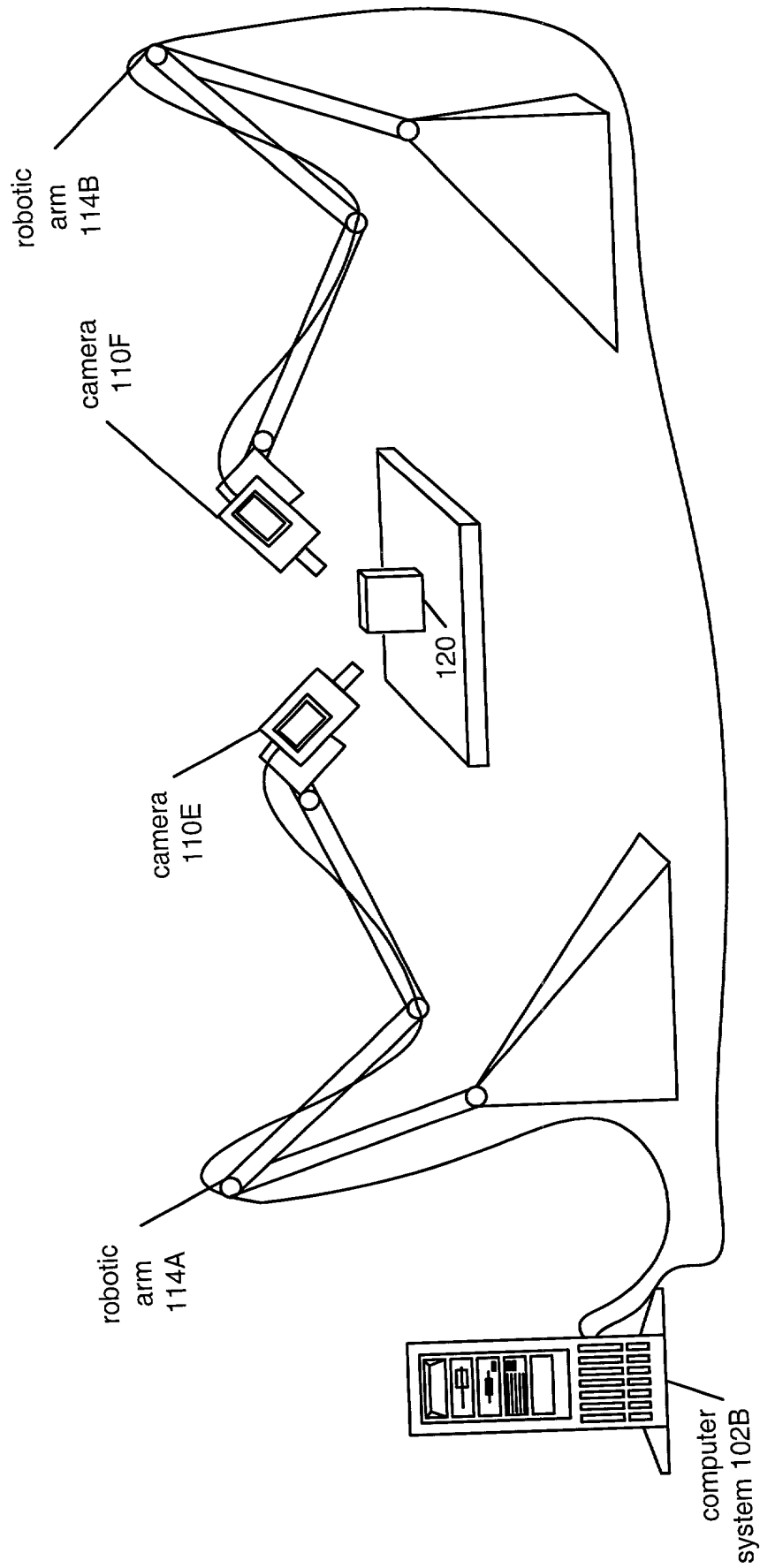


Figure 3B

FIG. 3C

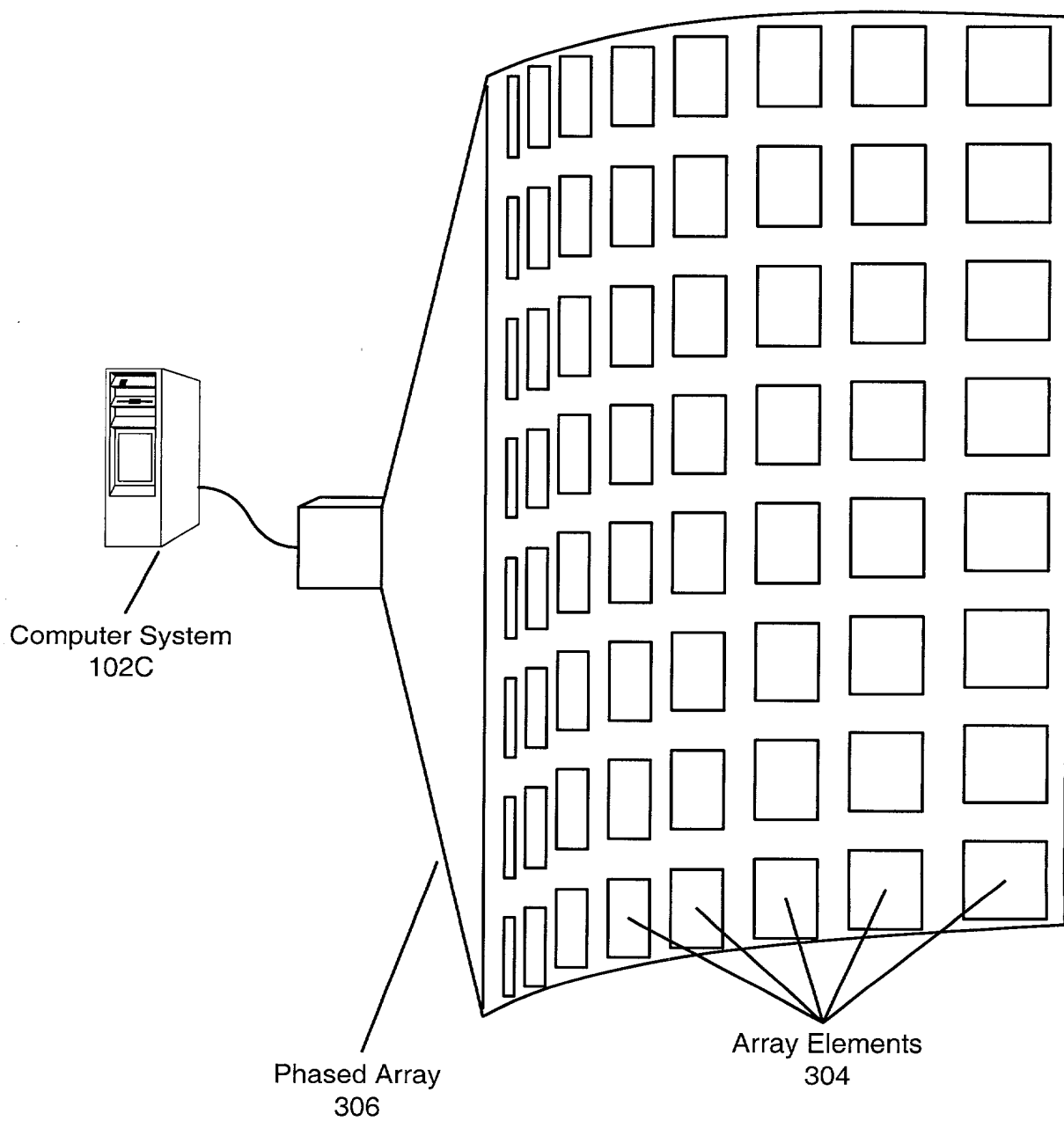


Figure 3C

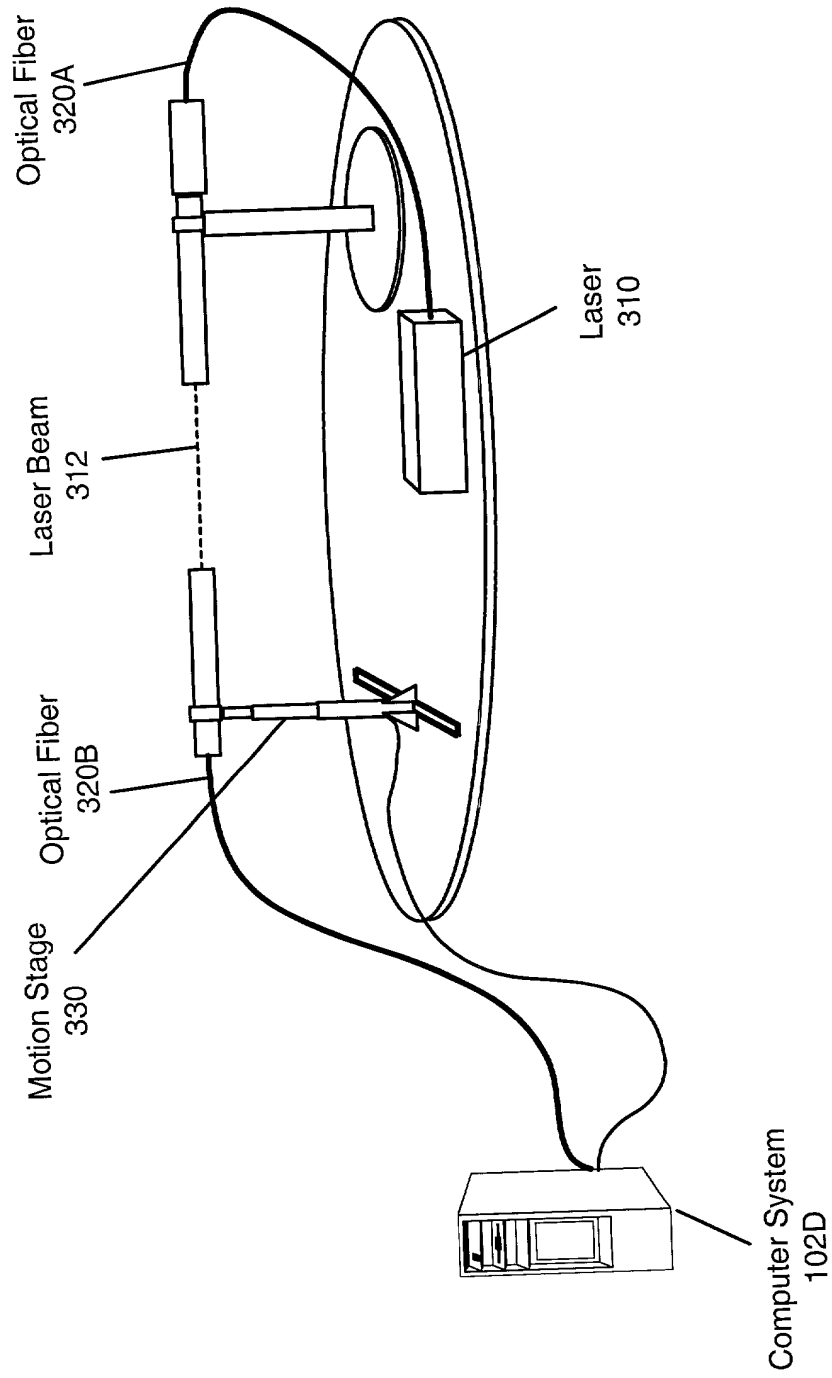
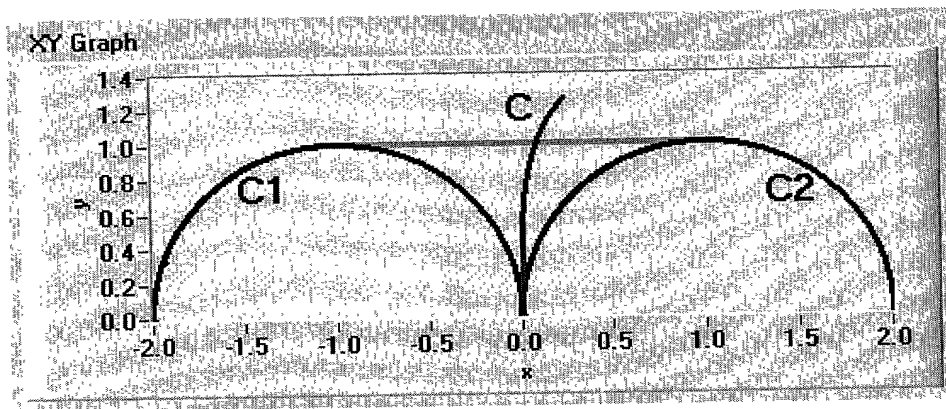
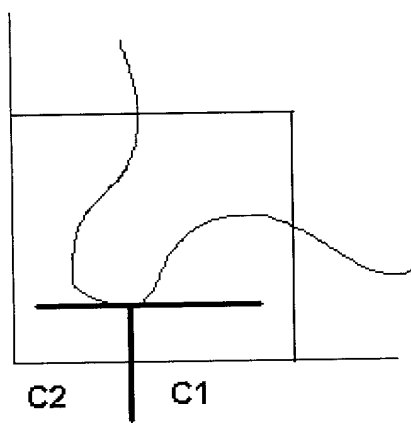


Figure 3D



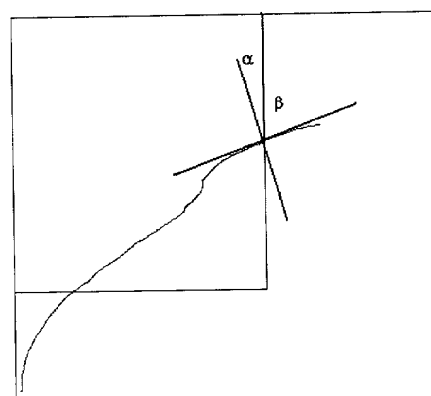
The situation of Lemma 1

Figure 4A



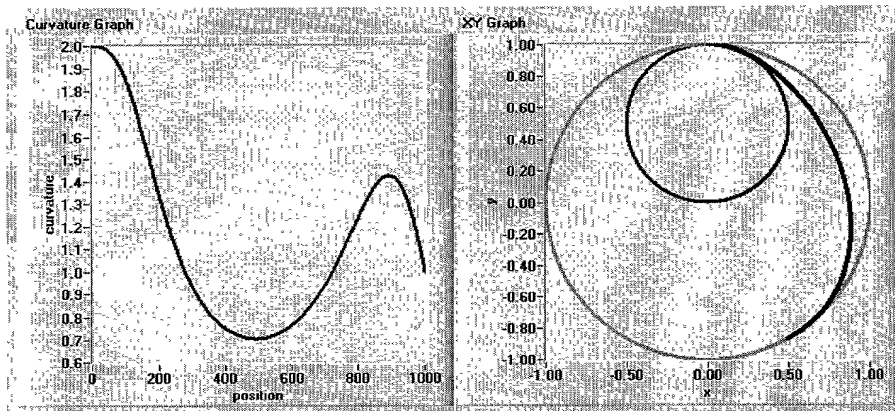
Case (A)

Figure 4B



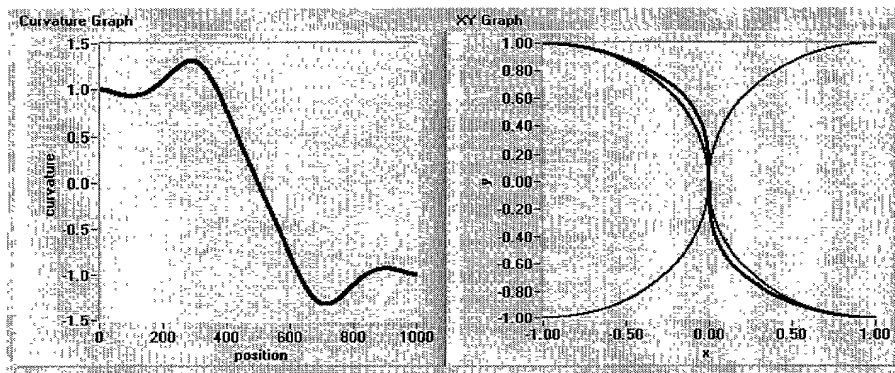
Case (B)

Figure 4C



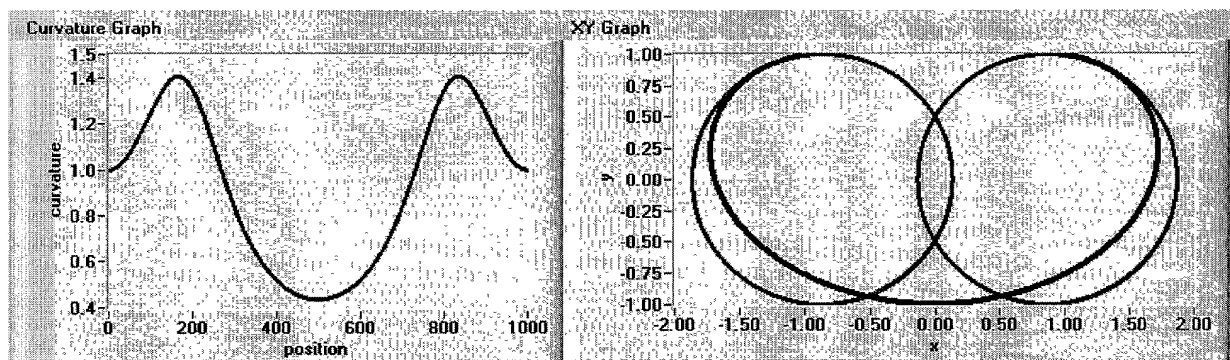
Smooth transition between two circles of different radii.

Figure 4D



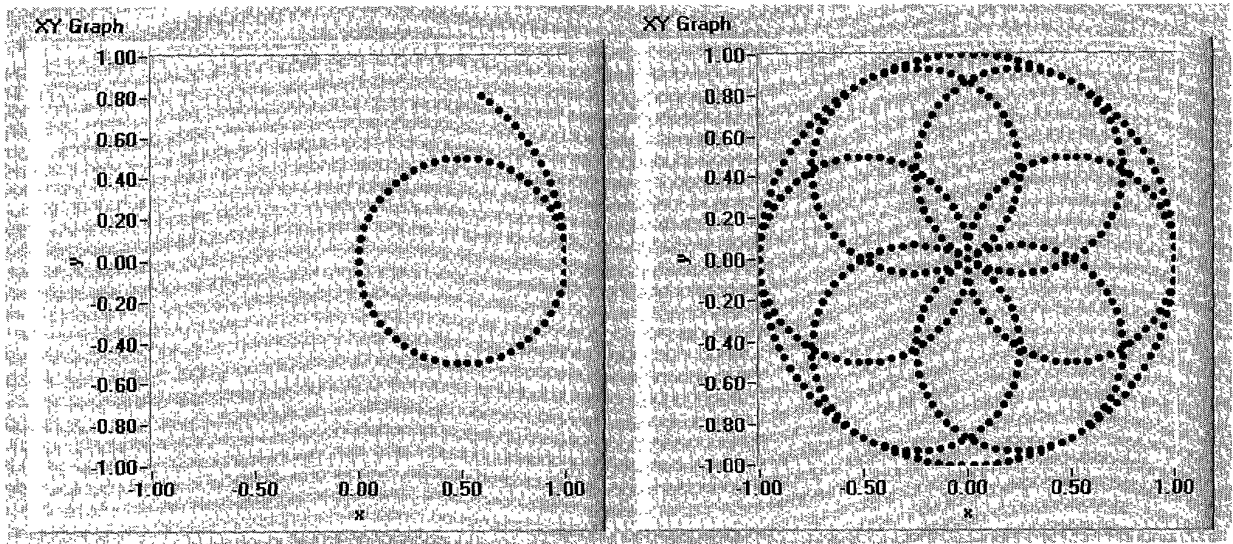
Smooth transition between two circles of same radius.

Figure 4E



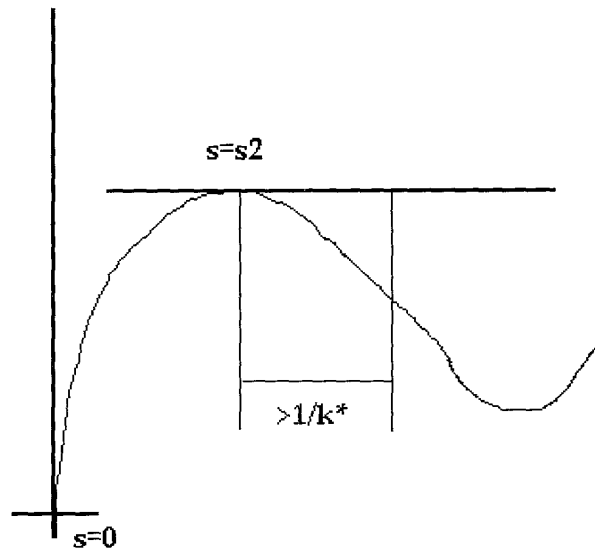
Transition between two unit circles of radius 1. The distance between the circles is $\sqrt{3}$

Figure 4F



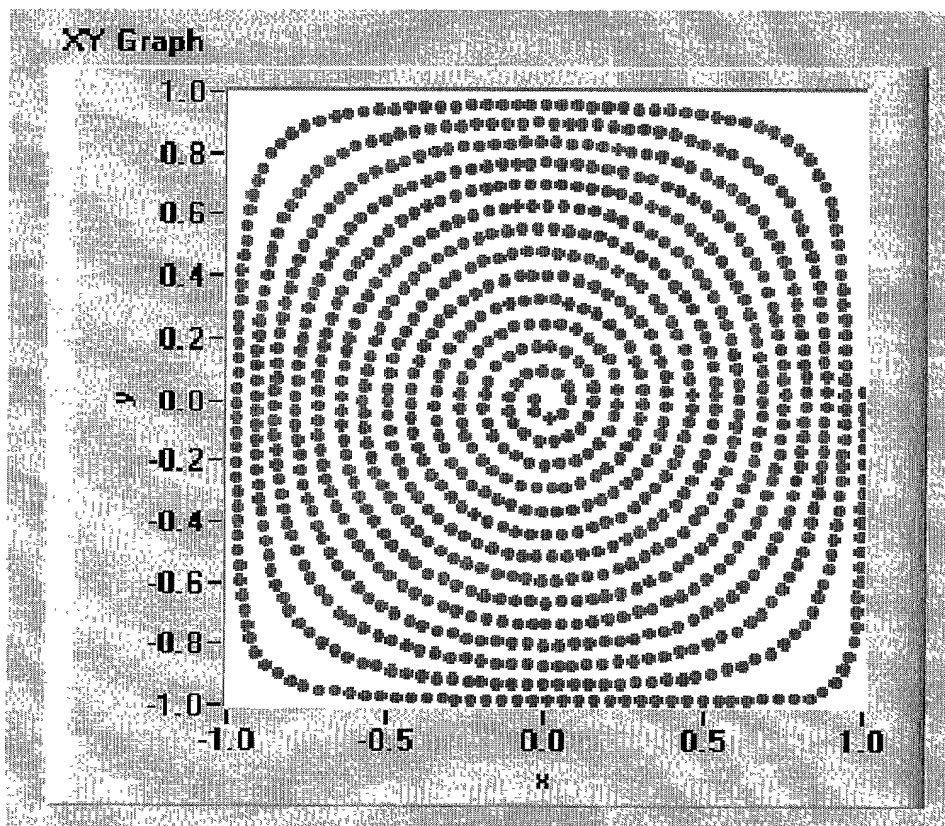
Beginning (left) and completion (right) of a scanning scheme where the curvature is below a certain value

Figure 5A



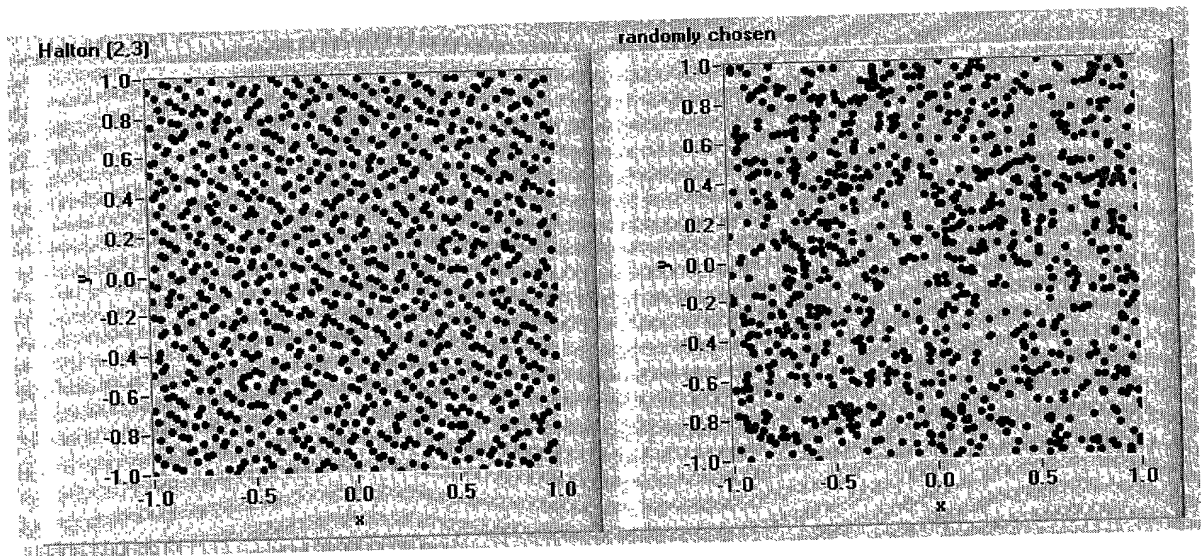
Construction of s_2 and the subsequent part of the curve

Figure 5B



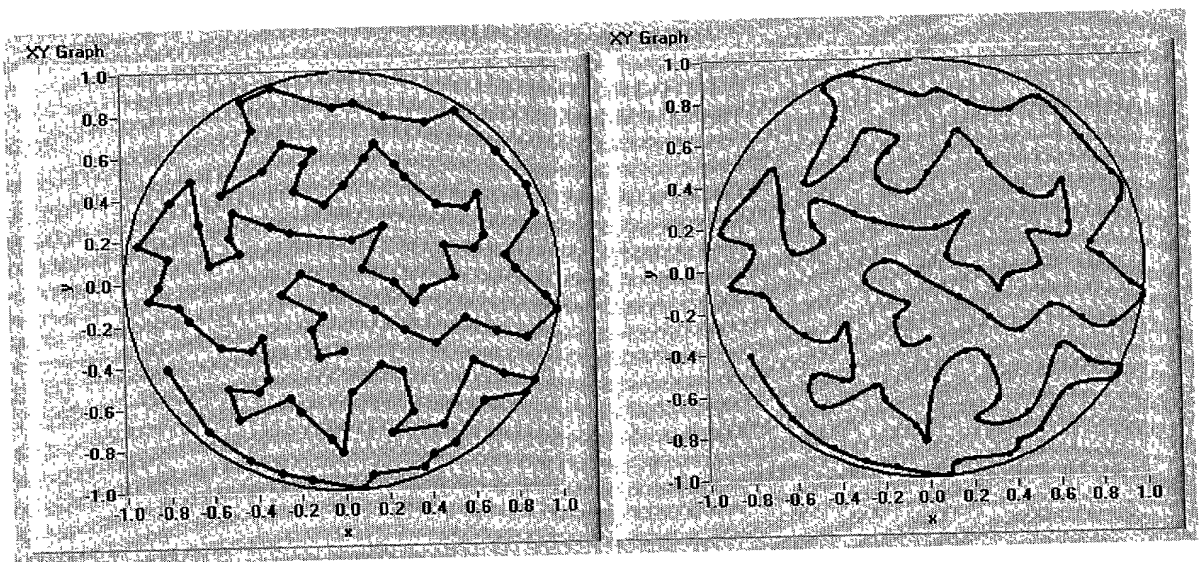
Conformal Spiral.

Figure 6



The first 1000 Halton points (left) and randomly chosen points (right)

Figure 8A



Original solution (left) and splined version (right).

Figure 8B

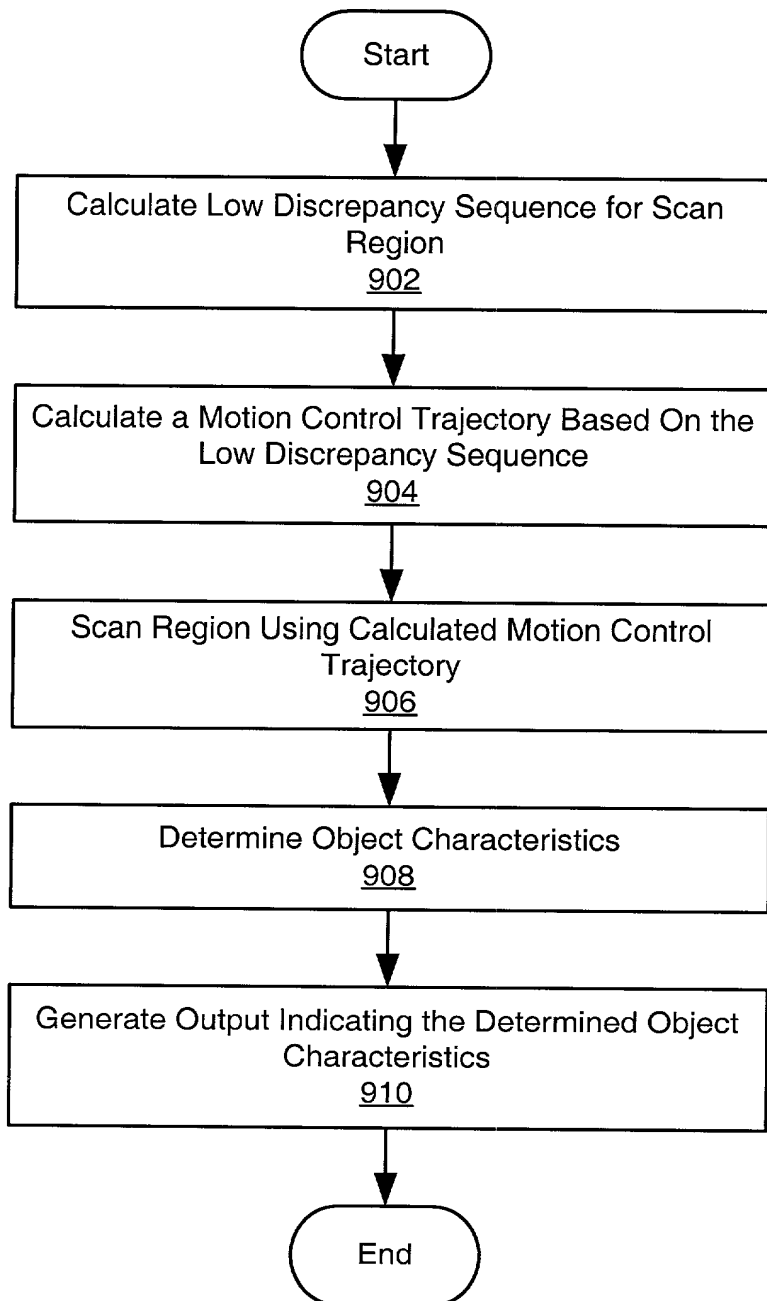
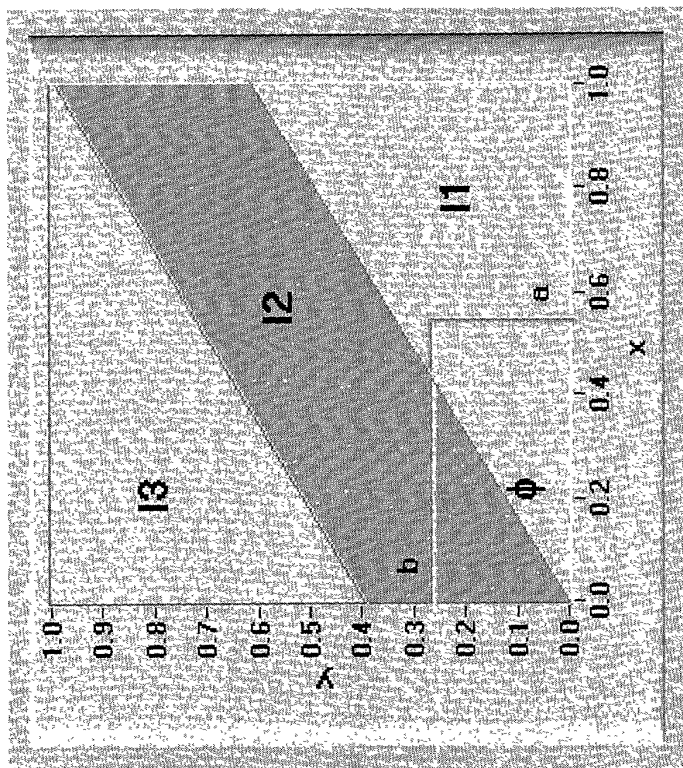


Figure 9



Definition of I_1 , I_2 , and I_3

Figure 10

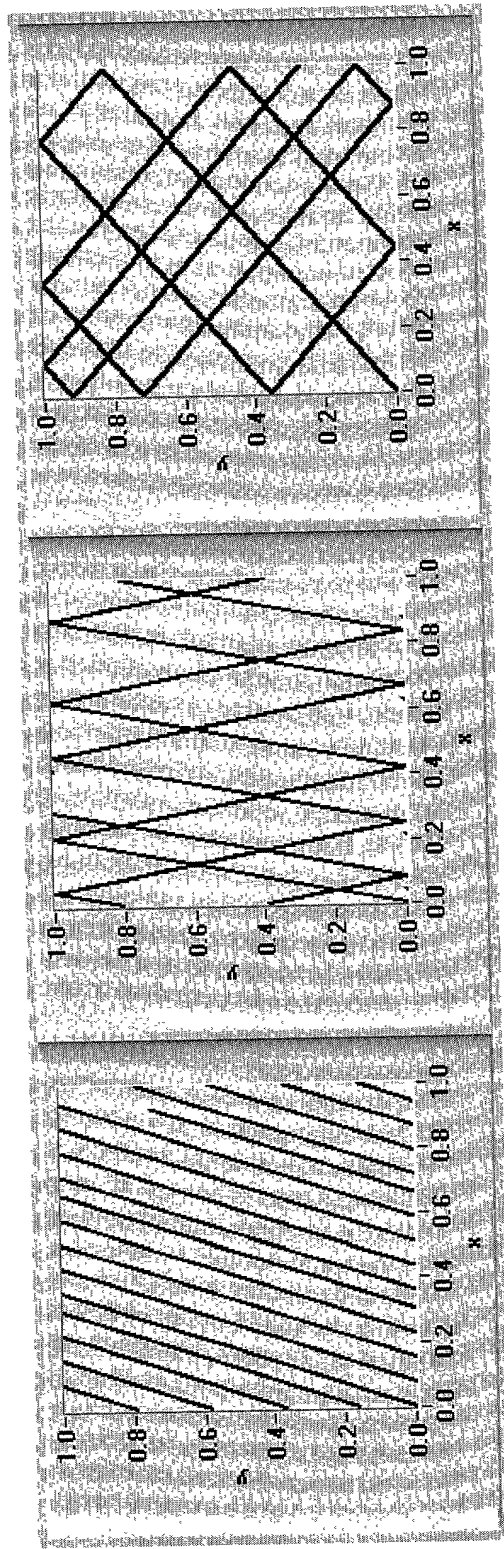


Figure 11C

Figure 11B

Figure 11A

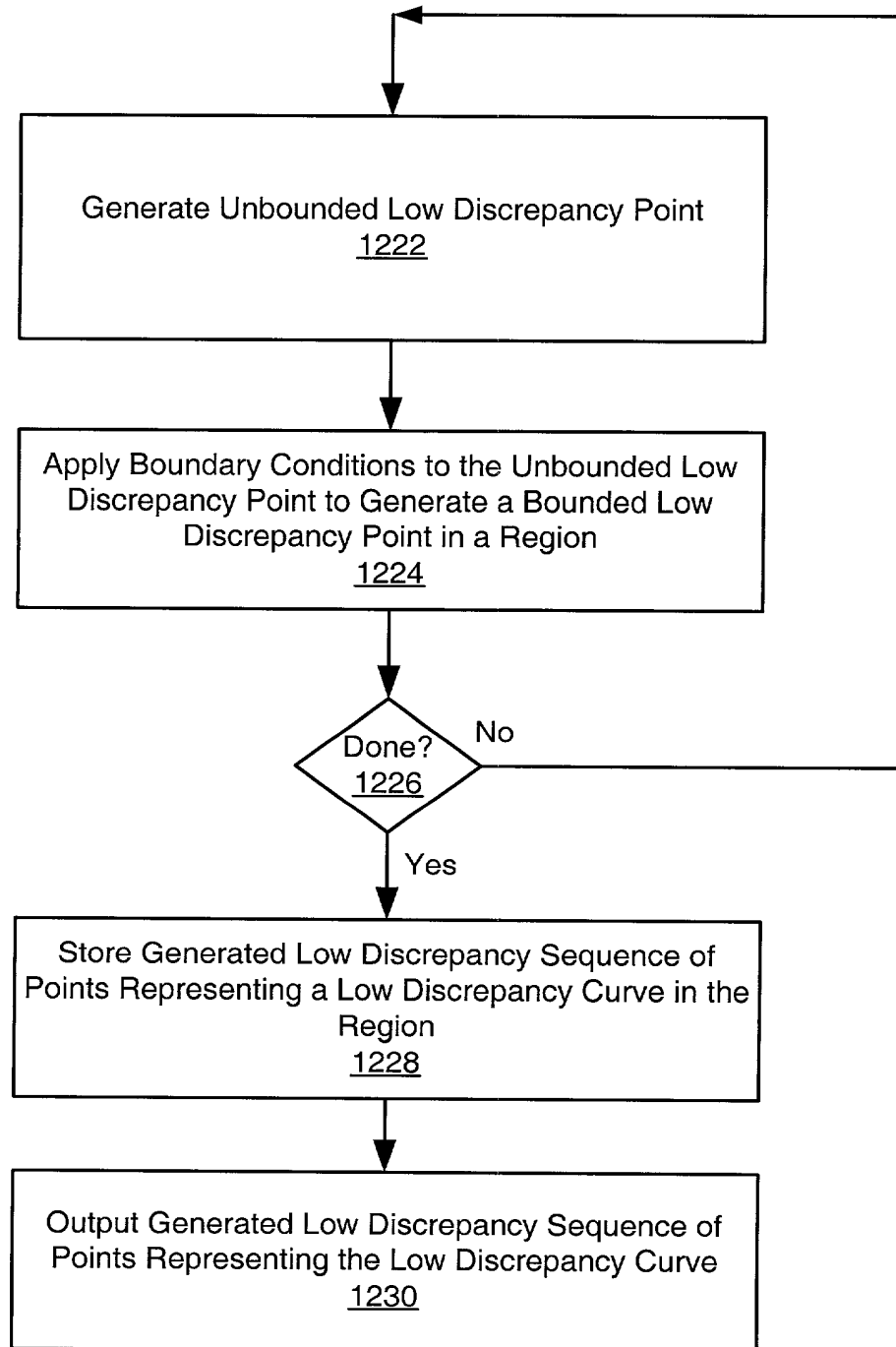


Figure 12A

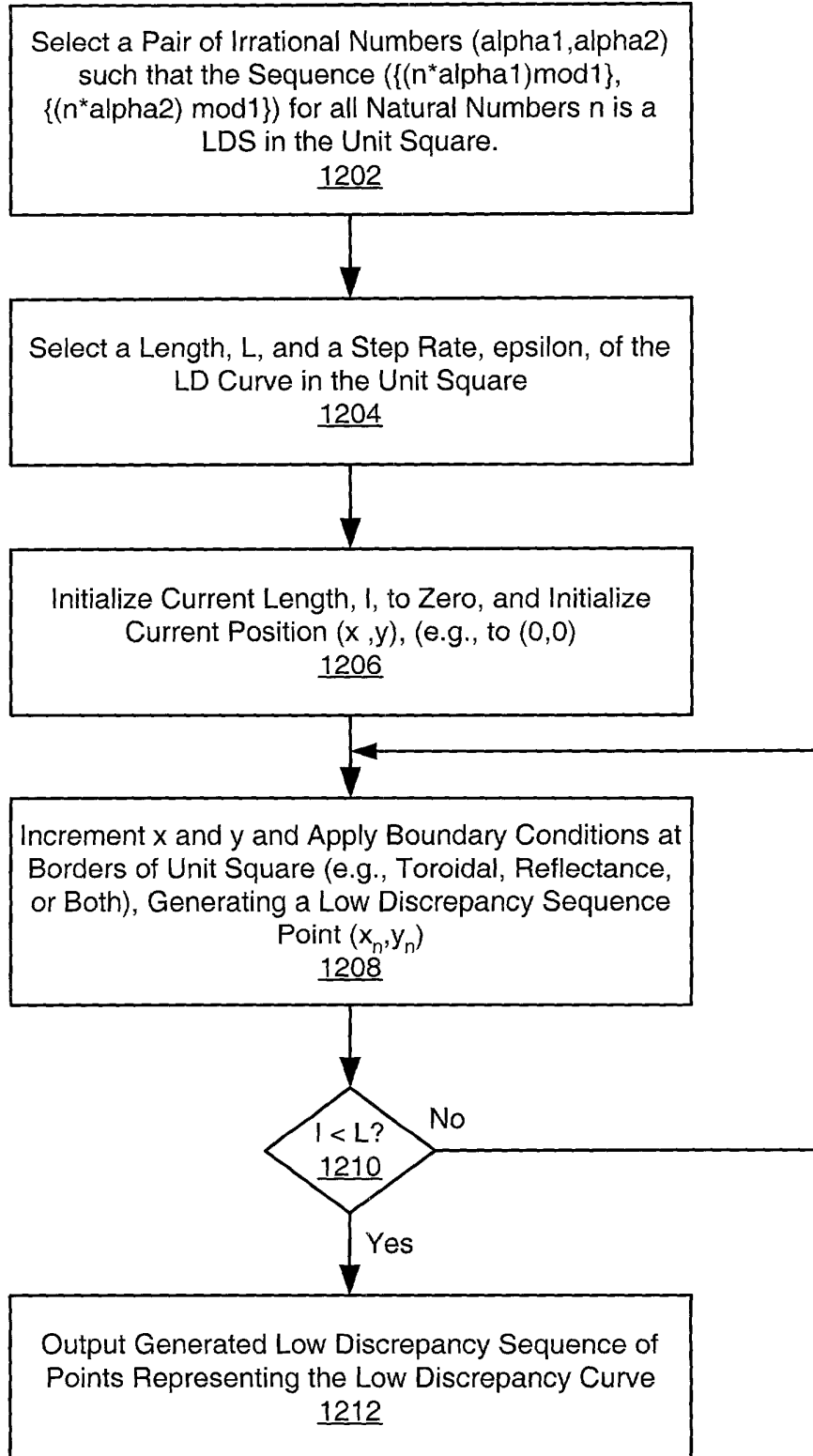
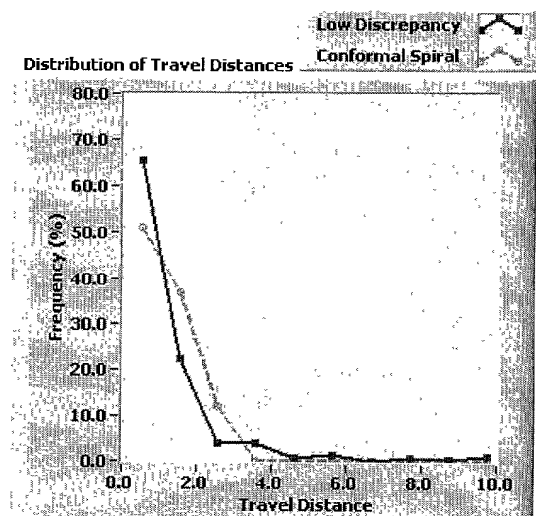


Figure 12B

Figure 13A

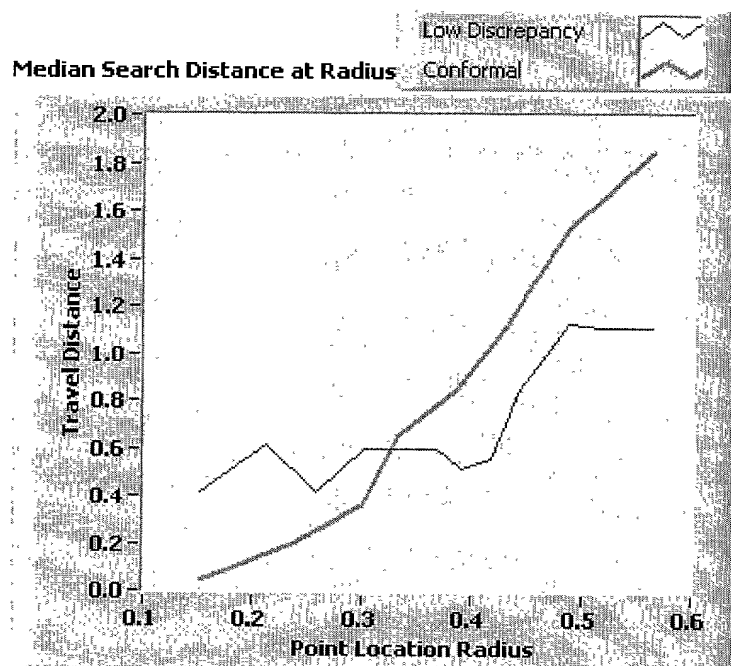


Figure 13B



Comparison of Conformal Spiral and Low Discrepancy Searching

Figure 13C



Comparison of Travel Distance for Low Discrepancy Search and Conformal Spiral Search

Figure 13D

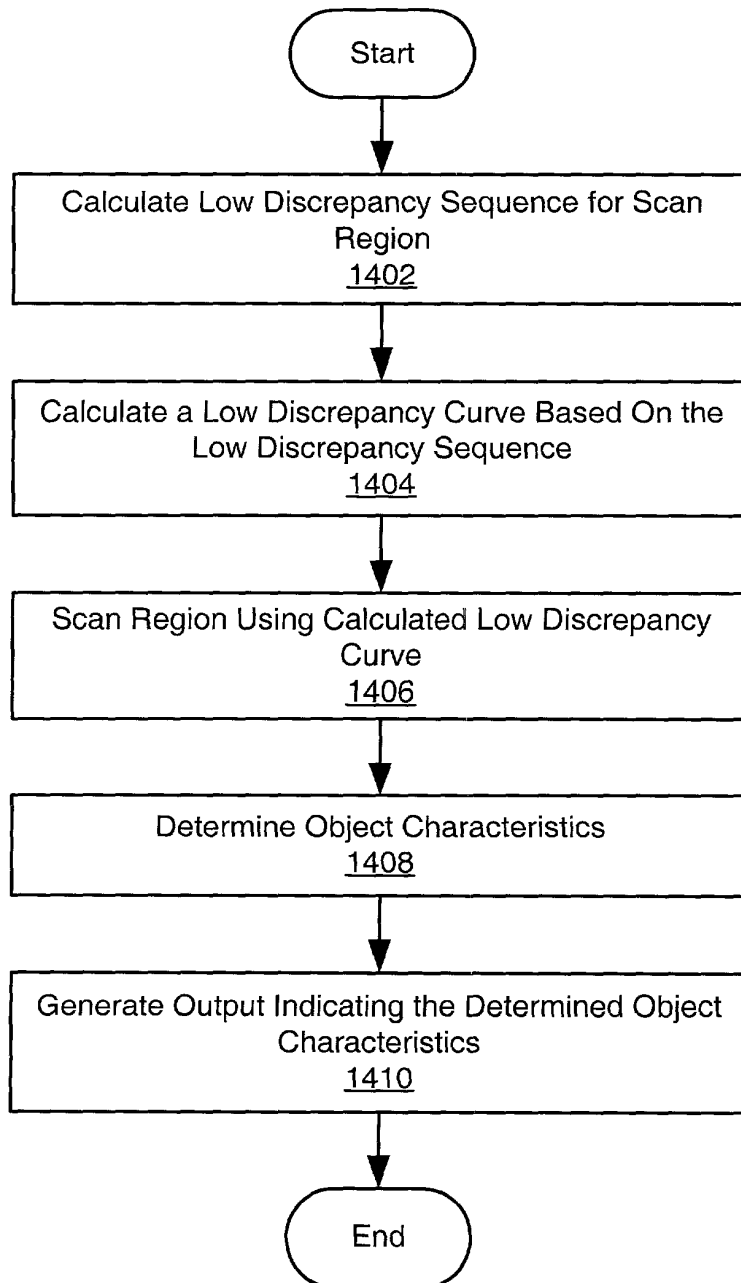
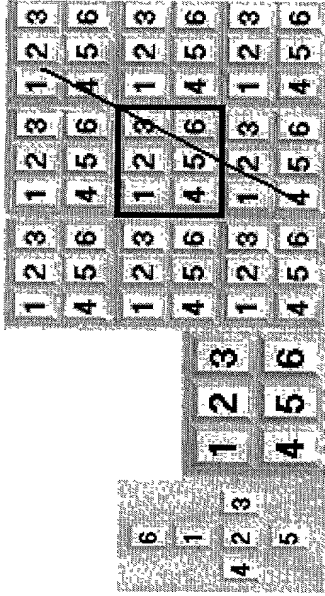
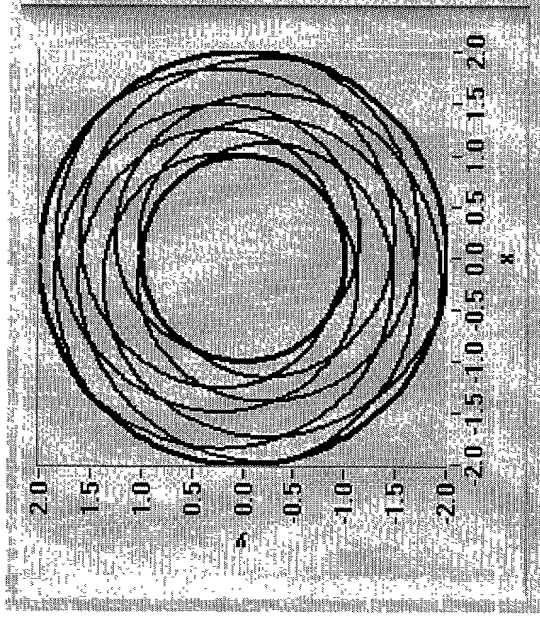


Figure 14



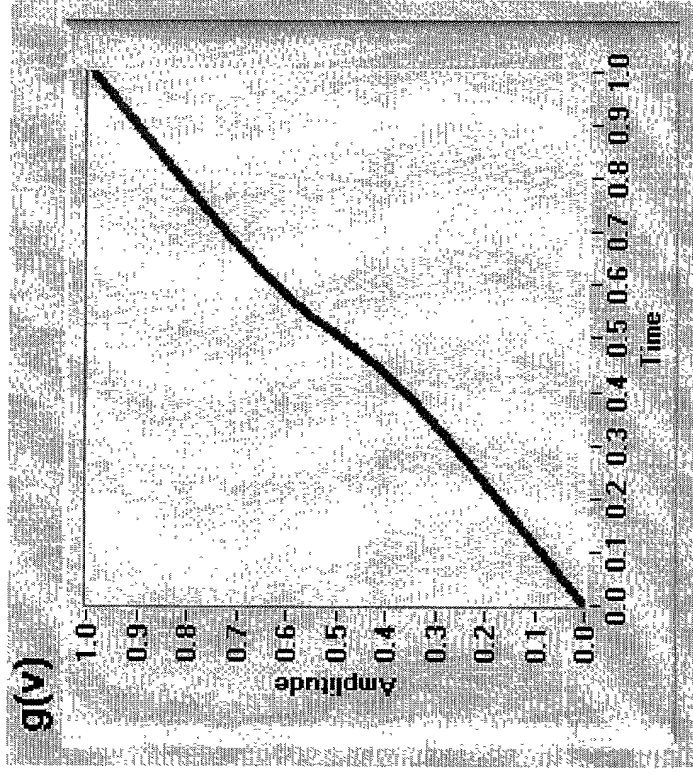
Tiling of the plane and relation to the surface of the unit cube



Low-discrepancy curve in a ring

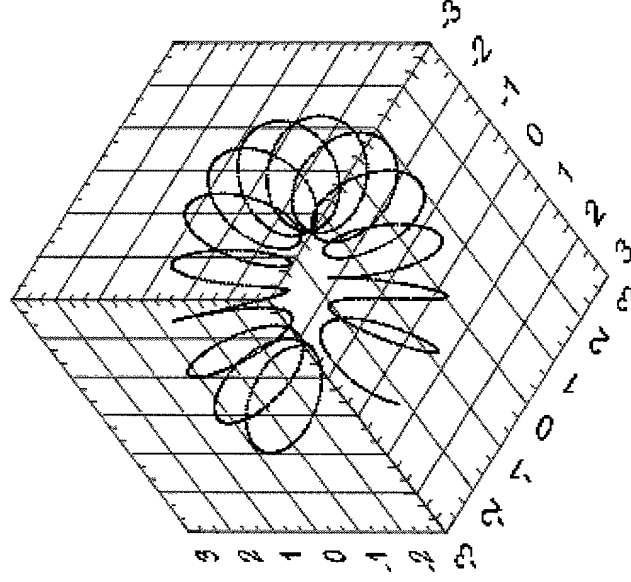
Figure 15A

Figure 15B



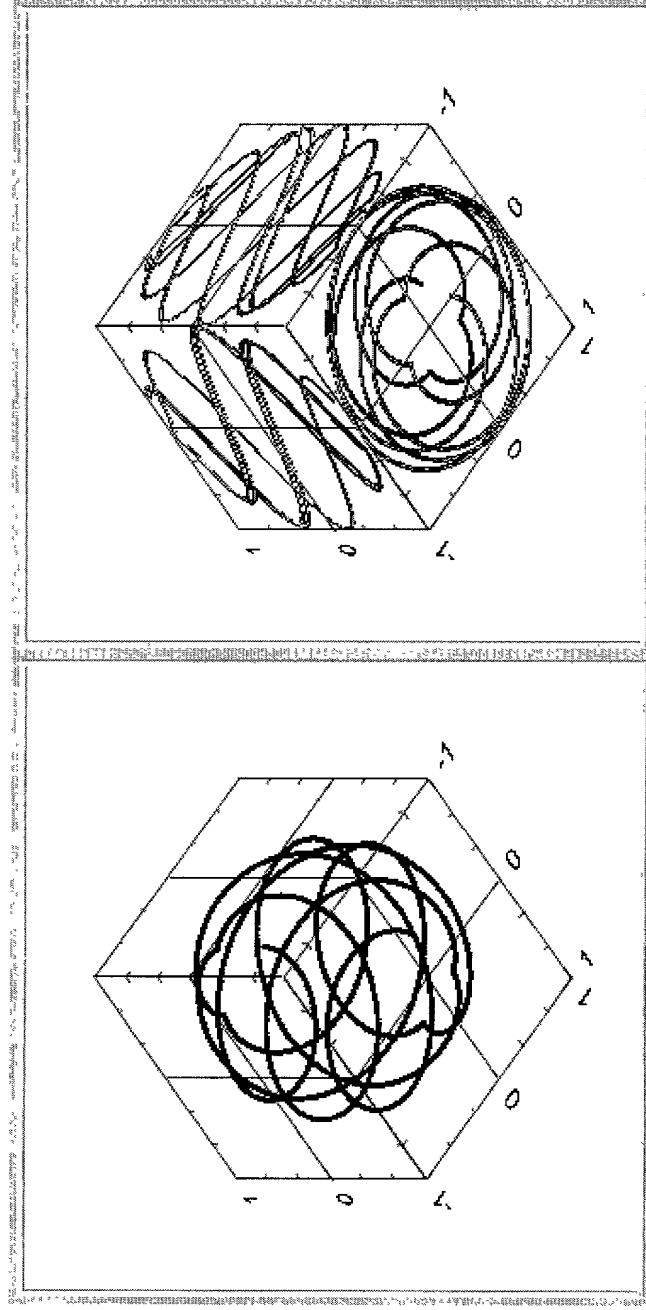
Low Discrepancy Preserving Mapping Function

Figure 15C



Low-discrepancy curve filling the surface of a torus

Figure 15D



Low-discrepancy curve on a sphere
(left) and projections (right)

Figure 16

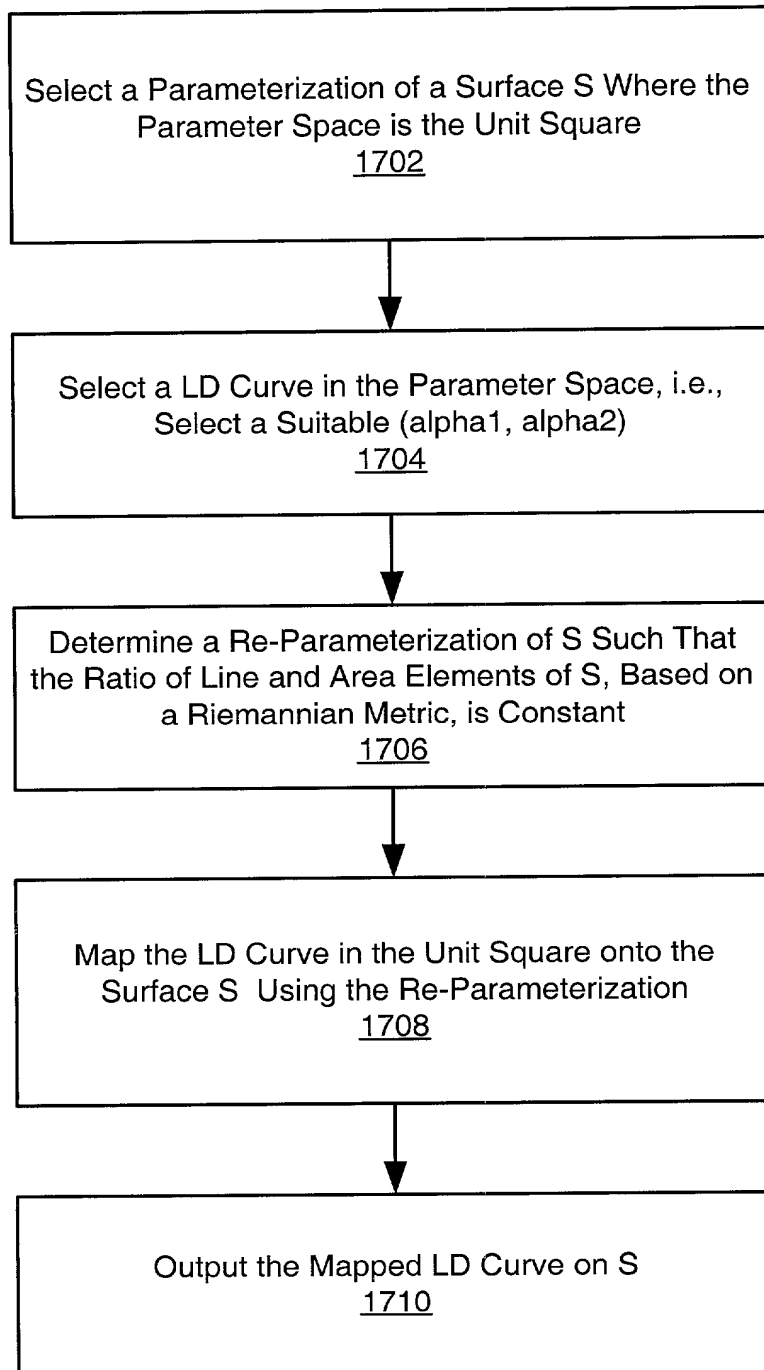
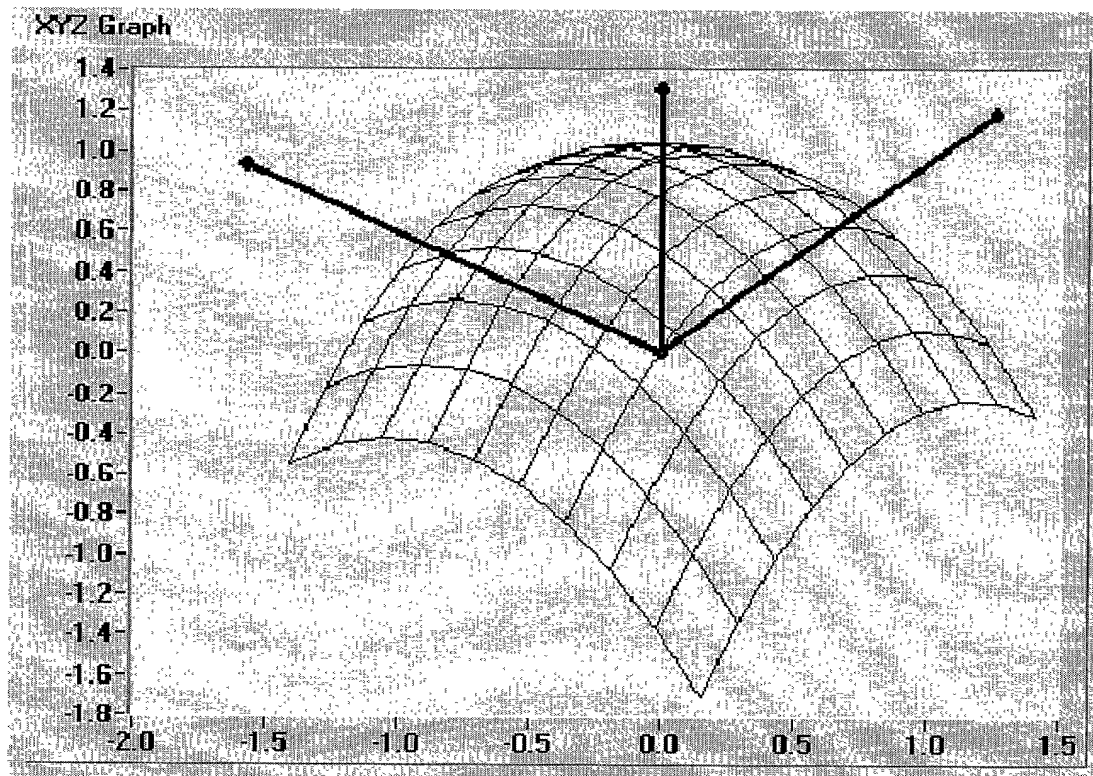


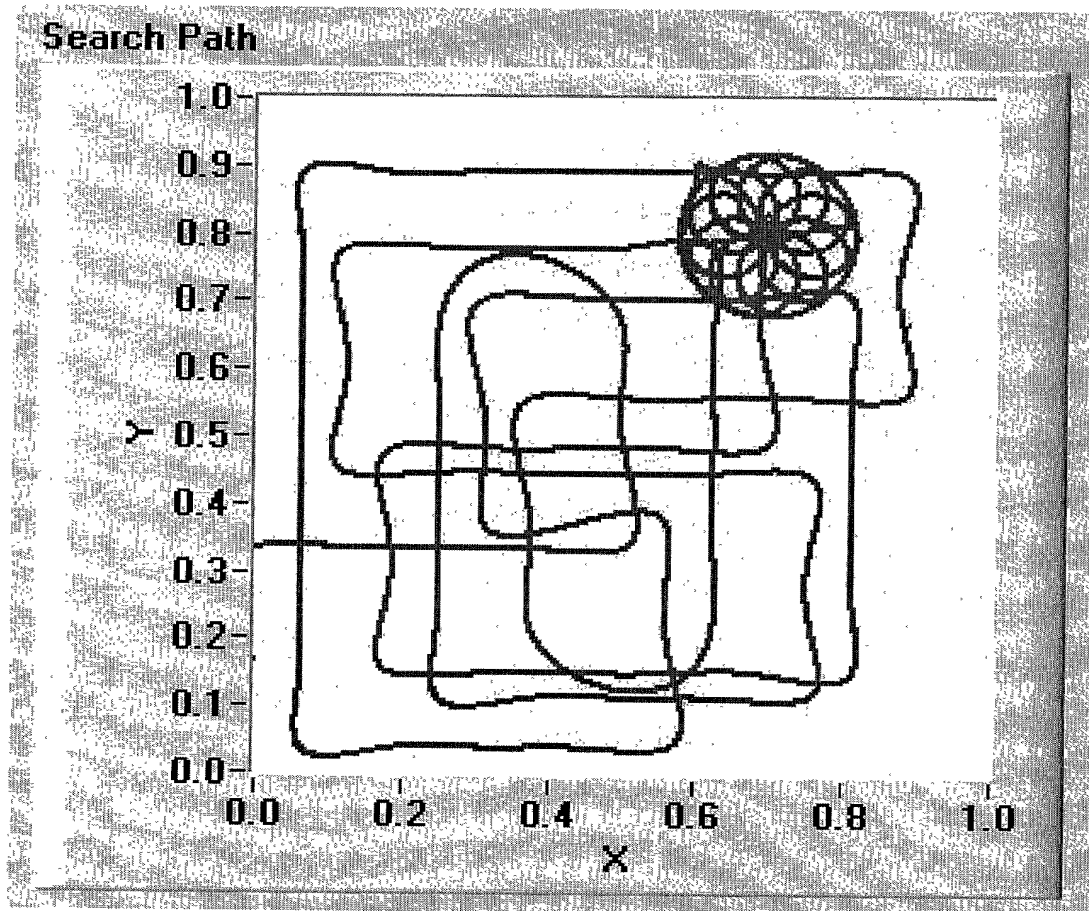
Figure 17



Surfaces can be scanned efficiently when the term low discrepancy sequence/curve can be generalized, e.g. based on metrics on the surface.

Figure 18

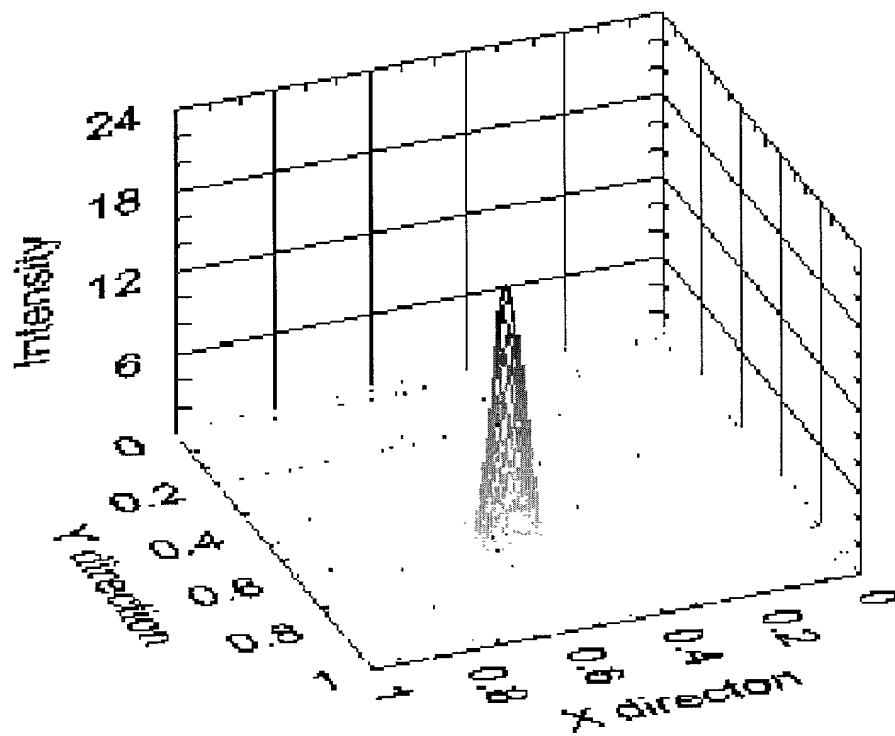
0987697.060304



Splined Low Discrepancy Curve coarse search with refined final approach

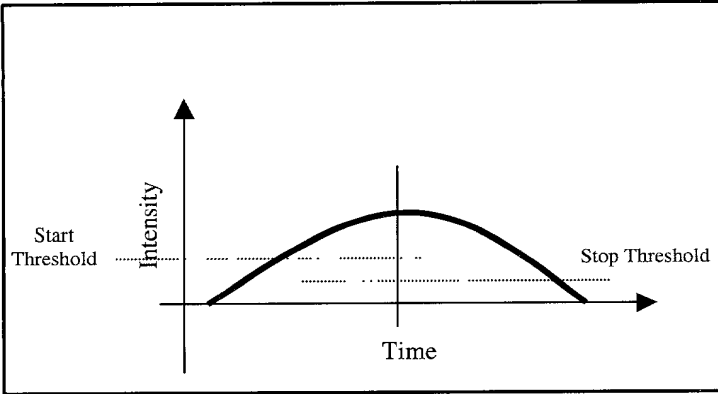
Figure 19

Intensity Field Distribution in Search Area

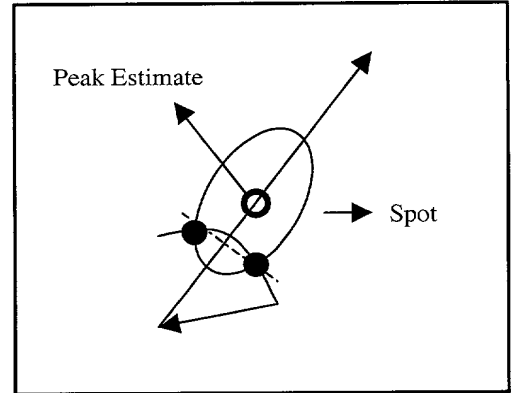


Beam intensity distribution in search area

Figure 20



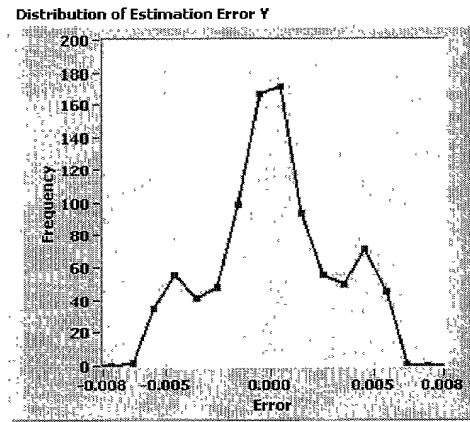
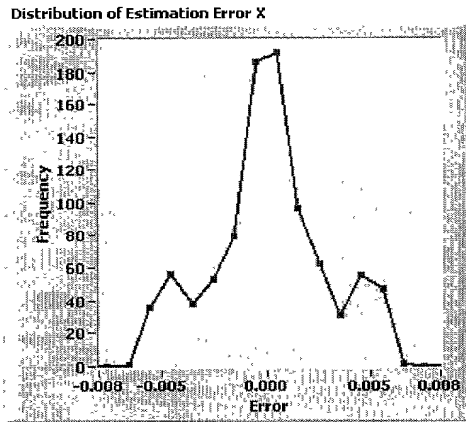
Location of the Peak



Initial Final Approach Move

Figure 21A

Figure 21B



Error distribution of the estimated peak X coordinate error (left) and Y coordinate error (right)

Figure 21C

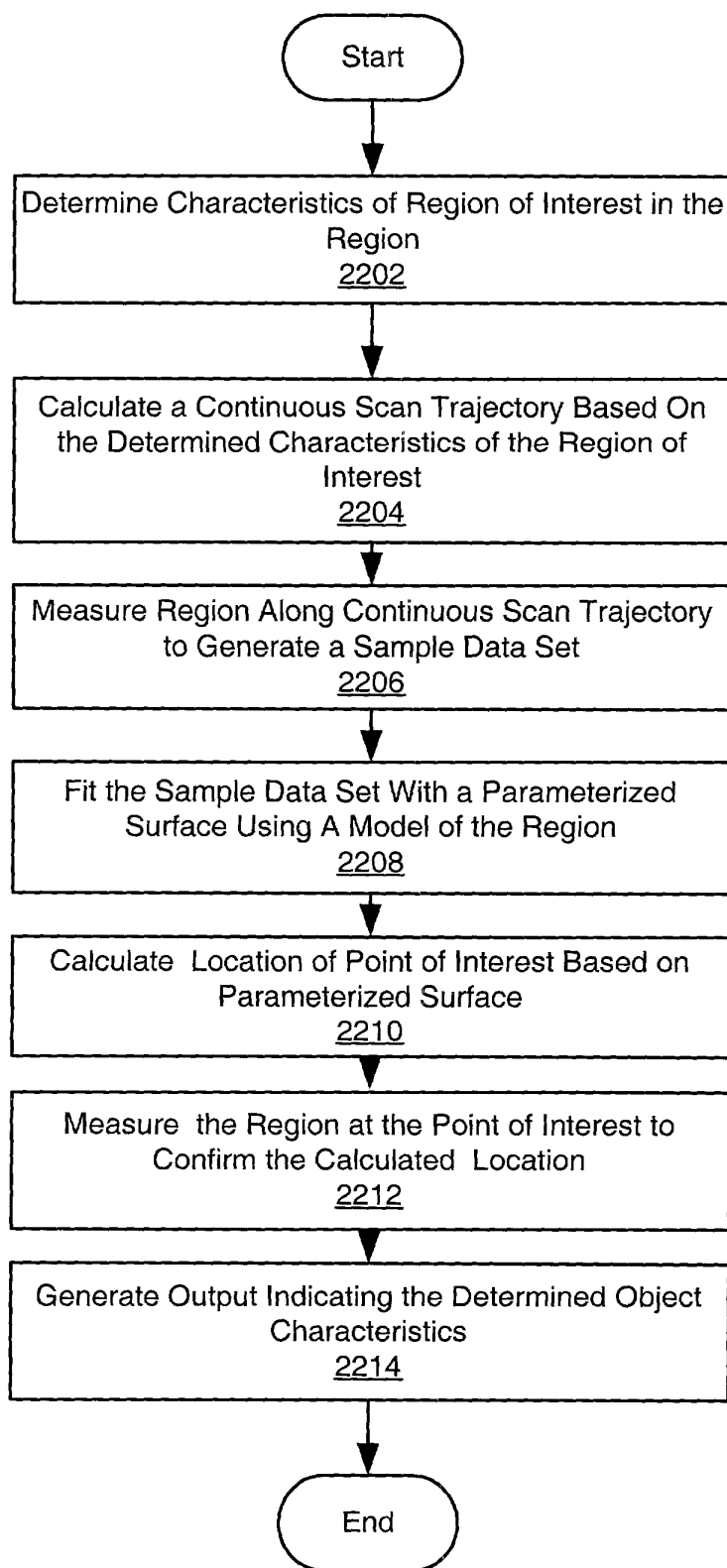


Figure 22

Figure 1. The effect of the concentration of the *Agrobacterium* suspension on the transformation efficiency of *Agrobacterium* strains. The transformation efficiency of *Agrobacterium* strains was determined by the number of transformants per 10⁶ cells. The data are the mean \pm SD of three independent experiments. The asterisk indicates a significant difference ($p < 0.05$) between the control and the treated groups.

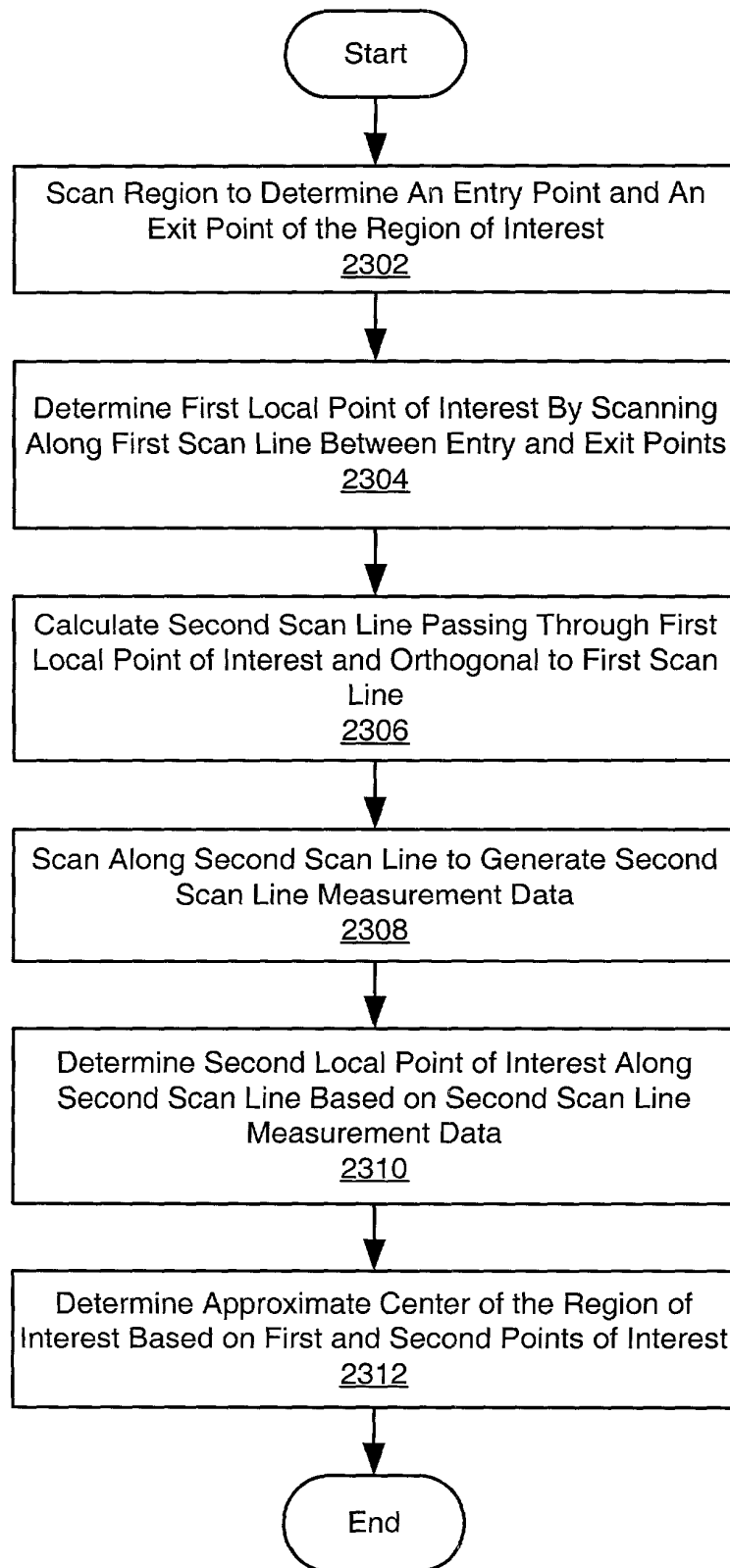


Figure 23